Structural Engineering and Mechanics, *Vol. 74, No. 2 (2020) 267-282*
DOI: https://doi.org/10.12989/sem.2020.74.2.267

Seismic assessment of thin steel plate shear walls with outrigger system

Ebtsam Fathy*

Structural Engineering Department, Faculty of Engineering, Zagazig University, Zagazig, Sharkia, Egypt

(Received August 2, 2018, Revised November 12, 2019, Accepted December 12, 2019)

Abstract. The seismic performance and failure modes of the dual system of moment resisting frames and thin steel plate shear walls (TSPSWs) without and with one or two outrigger trusses are studied in this paper. These structural systems were utilized to resist vertical and lateral loads of 40-storey buildings. Detailed Finite element models associated with nonlinear time history analyses were used to examine seismic capacity and plastic mechanism of the buildings. The analyses were performed under increased levels of earthquake intensities. The models with one and two outriggers showed good performance during the maximum considered earthquake (MCE), while the stress of TSPSWs in the model without outrigger reached its ultimate value under this earthquake. The best seismic capacity was in favour of the model with two outriggers, where it is found that increasing the number of outriggers not only gives more reduction in lateral displacement but also reduces stress concentration on thin steel plate shear walls at outrigger floors, which caused the early failure of TSPSWs in model with one outrigger.

Keywords: failure modes; seismic capacity; thin steel plate shear walls; moment resisting frames; outrigger trusses

1. Introduction

High-rise buildings have become a social necessity these days. “These buildings should include complete lateral and vertical-force-resisting systems capable of providing adequate strength, stiffness, and energy dissipation capacity to withstand the design ground motions within the prescribed limits of strength demand” FEMA450-1 (2003). Therefore, the designers always aim to develop and choose the appropriate and economical structural system for achieving these requirements. It is also common to use two or more structural systems in tall buildings to increase its efficiency such as frame-shear wall system and outrigger-frame-core system Gunal and Ilgin (2014). Outrigger is rigid beam or truss used to connect the core or internal shear wall with the perimeter columns at one or more levels along building’s height. This interaction between frame and shear wall by using outriggers increases the overall lateral stiffness of the building (Choi *et al*. 2013, Li and Wu 2004). At the same time, the outriggers and columns will resist rotation of the core or shear wall and thus reduce the lateral deformations of the building and the bending moments in the walls (Lee *et al*. 2013, Patil, and Sangle 2016, Fan *et al*. 2009, Zeidabadi *et al*. 2004, Brunesi *et al*. 2016, Hoenderkamp and Bakker 2003, Park *et al*. 2002).

Another economical and effective lateral load resisting system is thin steel plate shear walls, which showed increase usage in the last four decades. In this system, thin infill steel plates are connected to beams and columns (boundary elements). The mechanism of these walls is to buckle in shear forming tension field action that carrying shear forces and transmitted it to boundary elements. This mechanism has high ability to dissipate energy under lateral loads (Choi and Park 2008, Guo *et al*. 2013). Studying the effect of existing outrigger system on these walls is an important issue to find out the advantages, disadvantages, and the expected plastic mechanism because outriggers produces horizontal force acting on shear wall at its floors as well as it causes irregularities of structural rigidity along the building height (Choi *et al*., 2012).The importance of this study is that most recent seismic provisions require a suitable plastic mechanism under severe earthquakes to avoid brittle failure, such as (EN 1998-1 2004, FEMA-350 2000).

Seismic capacity and failure modes of buildings, verify by checking their performance through increased levels of earthquake intensity using experimental tests or numerical simulations. The results of experimental tests are reliable but limited to low-rise buildings or scale models of tall buildings (Kajiwara *et al*. 2009, Chung *et al*. 2010, Wu *et al*. 2016, Lu *et al*. 2016, Lu *et al*. 2012, Jiang *et al*. 2012, Ghannadi and Kourehli 2019). The reason for this limitation is the expensive cost of these tests and the lack of laboratories and large shaking tables that can check the collapse behavior of full-scale tall buildings. Numerical simulations proved that it is an important tool to make analysis, optimization, design, and could verify failure modes of different type of structures (Gantes et al. 2001, Civalek (2007), Civalek (2007), George *et al.* 2011, Lu *et al.* 2012, Jiang *et al*. 2012, Lu *et al*. 2016, Ashkezari (2018)). One of the most common methods for numerical simulation of the buildings is the finite element method. This method can check failure modes of the building by using detailed finite element model associated with adequate nonlinear analysis. Many studies have examined the nonlinear seismic performance and failure modes of tall buildings and skyscrapers by using FE models to make sure that these buildings would satisfy the safety requirements of

*Corresponding author, Ph.D.
E-mail: efsadik@gmail.com; efsadik@zu.edu.eg

http://www.techno-press.com/journals/sem&subpage=7
ISSN: 1225-4568 (Print), 1598-6217 (Online)

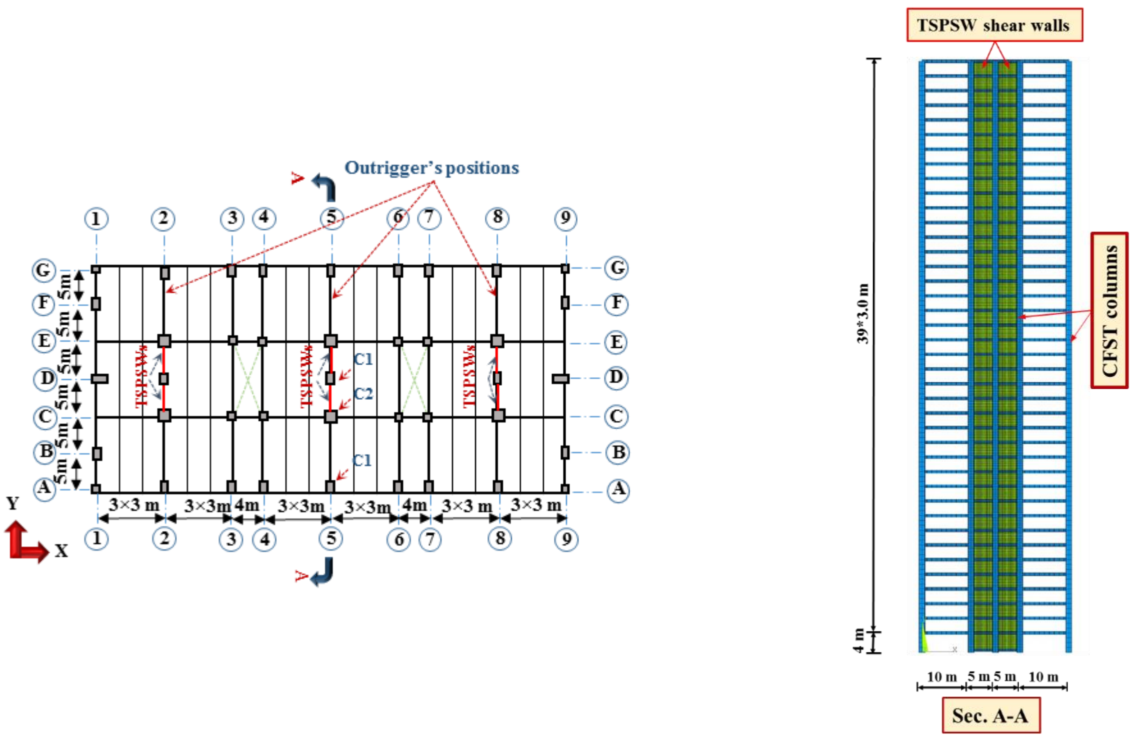

(a) (b)

Fig. 1 Geometric details of the buildings: (a) plan and; (b) elevation at section A-A

seismic provisions under severe earthquakes (Lu *et al.* 2016, Lu *et al.* 2012, Jiang *et al.* 2012, Epackachi *et al.* 2012, Lu *et al.* 2013, Li *et al.* 2014). Most of these Studies derived their results depending on a comprehensive investigation of a case study building and didn't focus on the effect of outrigger numbers and their positions on the failure modes of the buildings.

Therefore, this paper investigates the seismic capacity of the dual system of moment frames and thin steel plate shear walls with and without outrigger trusses. These structural systems used to resist vertical and lateral loads of 40-storey building. The first part represented the design of the building, optimum locations and depth of outrigger trusses for the second and third cases and linear responses under the design basis earthquake (DBE) using SAP2000 v15 (2010). Accordingly, detailed finite element models were established to simulate the considered structural system using ANSYS 15.0 software (2013). Nonlinear time history analysis performed under increased levels of earthquake intensities until the stress of any part of the models reached its ultimate value. The results demonstrated plastic mechanism and seismic capacity of each case, which indicate that, the outrigger numbers along the building height have a great influence on failure modes of the considered structural system.

2. Building design description

2-D models of frame-thin steel plate shear wall with different numbers of outrigger trusses were utilized in this study. The 2-D model extracted from 40-storey building as shown in Fig. 1. The building has a total height of 121 m with a storey area 62 ×30 m^2. The external mega columns are rectangular concrete-filled steel tubular (CFST) columns. The slabs were composite metal deck slab with thickness 110 mm. The structural system consists of multi thin steel plate shear walls (TSPSWs). Where, the CFST columns used for the moment resisting frames and forming the vertical boundaries of (TSPSWs). While the steel beams of the frame forming the horizontal boundaries of TSPSWs. Beam to column connections were assumed to be rigid. The building assumed to be constructed in seismic zone area with PGA equals 0.25g for the design basis earthquake (DBE) with return period 475 years. The building was designed in accordance with the EN 1998-1 (2004). Capacity design rules were adapted to get suitable plastic mechanism. Wherefore, the relation between the sum of resistance moments of columns (∑Mrc) and beams (∑Mrb) at every beam-column joint fulfills Eq. (1).

$$\sum Mrc \geq 1.3 \sum Mrb \tag{1}$$

The loads considered in the design were: dead load (G), live load (Q) and seismic load (E). The loading combinations in accordance with EN 1990 (2010) were as follows:

$$1.35G + 1.5Q \tag{2}$$

and

$$1.0G + \psi Q \pm 1.0E \tag{3}$$

Where, the combination coefficient of live load ψ was taken equal to 0.3. Under these loads, the beams, special plate shear walls TSPSW, external CFST columns, and outrigger trusses were designed as described in the next subsections.

Table 1 Designed Sections of elements and their mechanical properties

	Floor	Profile (mm)	Grade
Columns C1	1-10 11-20 21-30 31-40	1200x800x60 1200x800x55 1200x800x50 1200x800x45	Steel S450 Infill material C40/50
Columns C2	1-10 11-20 21-30 31-40	1200x1200x60 1200x1200x55 1200x1200x50 1200x1200x45	Steel S450 Infill material C40/50
Beams		HEA600	S275
TSPSWs web plate (clear distances)	1 2 -10 11 -20 21 -30 31-40	3800 x 3410 x 12 3800 x 2410 x 12 3800 x 2410 x 11 3800 x 2410 x 10 3800 x 2410 x 9	S275
Outriggers (horizontal members)	In the designed location	HEM 900	S450
Outriggers (Inclined members)	In the designed location	HD 400x463	S450

2.1 CFST Columns design

The CFST columns have many advantages where they can withstand large compressive loads due to the concrete confinement occurred by steel tube. In addition, the presence of concrete infill reduces the occurrence of local buckling of steel tube (Du *et al*. 2016, Du *et al*. 2016, Liew *et al*. 2016, Du *et al*. 2017). These columns were designed in accordance with EN 1994-1-1 (2004), which take account of second-order effects such as geometrical imperfections, local instability, cracking of concrete, and yielding of structural steel. According to that, CFST columns were checked at the ultimate limit state for: geometric limits of the steel sections against local buckling under compression, resistances of cross-sections and members to internal forces and moments, buckling resistance of the members, depending on their effectiveness slenderness, and local resistances to shear forces between steel and concrete. With this design method, the failure modes due to local buckling whether in column members or in skin of steel tube will be prevented. The expected failure modes, if the loads exceeded largely the design loads will be due to yielding of steel or crushing of concrete. The designed cross sections of CFST columns along the height of the building and their mechanical properties are listed in Table 1.

2.2 Design of TSPSWs

Thin steel plate shear walls (TSPSWs) are one of recent developments to resist seismic loads where the infill plate works as structural fuse under severe earthquakes. The efficiency of these walls is examined in this study without and with different numbers of outrigger trusses, where, the structural system of the considered buildings consists of moment resisting frames and TSPSWs. The walls consist of dual steel plate shear wall system as shown in Fig. 1 (b). These walls contain steel infill plates restricted by columns (vertical boundary elements (VBEs)) and beams of the floors (Horizontal boundary elements (HBEs)). The web plate allowed to buckle in shear forming diagonal tension-field which leading to dissipation of energy (Gholipour and Alinia 2016, Meng *et al*. 2015, Wang *et al*. 2015, Youssef *et al*. 2010, Guo *et al*. 2015, Zirakian and Zhang 2015, Hosseinzadeh and Tehranizadeh 2014, Purba and Bruneau 2015). This behaviour makes it suitable to resist seismic loading. Moreover, when the steel plate damaged during an extreme earthquake, it can be easily replaced with a reasonable cost and the building restore its whole efficiency. The boundary elements were designed to resist the yielded capacity of the plates and behave elastically except plastic hinging expected at the ends of HBE. The Canadian Standards (CAN/CSA S16-09 2009, FEMA 450 2003 and the ANSI/AISC 341-10 2010) provided design clauses for TSPSW with steel plate allowed to buckle in shear and develop tension-field action. FEMA 450 (2003) recommended that the aspect ratio of panel satisfies the following relation:

$$0.8 < \frac{L}{h} \le 2.5 \tag{4}$$

Where L is the bay width and h is the story height. The walls were in Y-Z direction and consist of dual TSPSW shear walls, each one has panel area equal 5.0*3.0 m^2 for typical floors and 5.0*4.0 m^2 for the first one. The infill plates are fully welded to the surrounding boundary elements. This system is designed to achieve a suitable aspect ratio for panel according to Eq. (4). In addition, with this arrangement for beams and vertical columns, the vertical load can transmit easily. Moreover, using dual TSPSW reduces the flexural forces of the boundary elements. The dual TSPSW shear walls were designed according to ANSI/AISC 341-10 (2010), which provides detailed design for web plate thickness and boundary elements limitations based on the capacity design principle. The thickness of thin plates varies from 12 mm to 9 mm along the building height as shown in Table 1. Accordance with this design, the expected failure mode of TSPSWs are mainly yielding and fracture of infill plates as a result of repeating inelastic buckling during development of tension field action under severe earthquakes. Plastic-hinges may also occur at the ends of horizontal boundary elements (HBEs). These failure modes were observed in the past experimental studies (e.g. Purba and Bruneau 2014, Vian and Bruneau 2005, Behbahanifard *et al*. 2003, Choi and Park 2009, Vatansever and Yardimci 2011 and Guo *et al.* 2015)

2.3 Optimum position of outrigger trusses

For the second and third models, supplementary stiffness system has been added by using one and two outrigger trusses respectively. The efficiency of outrigger system is influenced mainly by their location and their stiffness (Choi *et al*. 2012). Therefore, many studies have been done to find out the optimum position of outriggers, but their results were slightly different or they gave a range for the outrigger location in the building (Patil, and Sangle 2016, Zeidabadi *et al*. 2004, Lee and Tovar 2014, Hoenderkamp 2008, Zhou *et al*., 2016). Thus, to find exactly the optimum location of outrigger trusses for the considered building, the position of outrigger trusses was studied using linear time history analyses for both cases with one and two outrigger trusses using seven different earthquake records to certify the results. The peak ground acceleration (PGA) of the selected earthquakes was normalized to 0.25g to represent the design basis earthquake (DBE) of the construction area of the considered building. Table 2 summarizes the characteristics of the earthquake records used in this paper. The analyses were conducted using SAP2000 v15 (2010) which gives adequate results in linear analysis with reasonable time for the analysis. The response parameters of interest were lateral displacement index, which are imperative for tall buildings. For building with one outrigger truss, it was easy to find the optimum position of outrigger truss that gave the minimum lateral displacement. Where, forty analyses were done for each earthquake by changing the location of outrigger and finding the results of each case. After that, the average was taken from the results of the selected earthquakes. It is found that, the optimum position in case of using one outrigger for the second model was on the 22nd floor, which represented 55% of the building height measured from its base as shown in Fig. 2. This position achieved reduction in lateral top displacement reached 16.3%. It has been observed that, the presence of one outrigger in the first quarter of the building gives insignificant reduction in lateral displacement where, the improvement has not exceeded 5%. After that the effect of one outrigger began .to appear as shown in Fig. 2

To find the optimum position for two outrigger trusses in the third building, it needed 1600 cases for analysis for each earthquake reduced to 800 cases due to that the results forming symmetrical matrix. Then the average results for all earthquakes are calculated. Fig. 3 shows the relation between the position of 1st outrigger truss and 2nd outrigger truss versus the average reduction ratio in lateral top displacement. It is found that, the optimum positions of two outrigger trusses that achieve the minimum lateral top displacement are at the13th and 27th stories which represented 33.33% and 66.67% of building height measured from its base. These positions for the two outrigger trusses achieve average reduction in lateral displacement equals 24.4%. According to these results the position of outrigger truss is at the 22nd floor in the second model and at the 13th and 27th floor for third model.

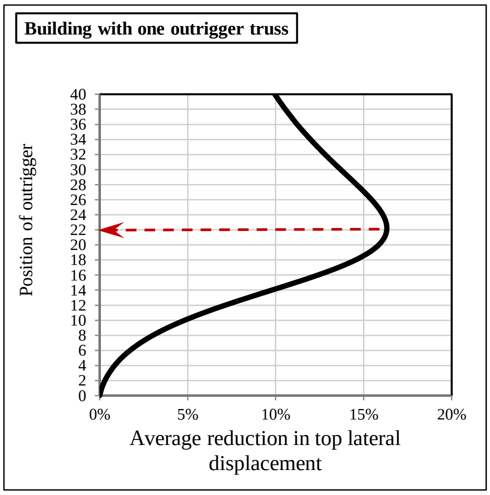

Fig. 2 Average reduction in top lateral displacement extracted from seven earthquake records versus the change in the position of one outrigger truss

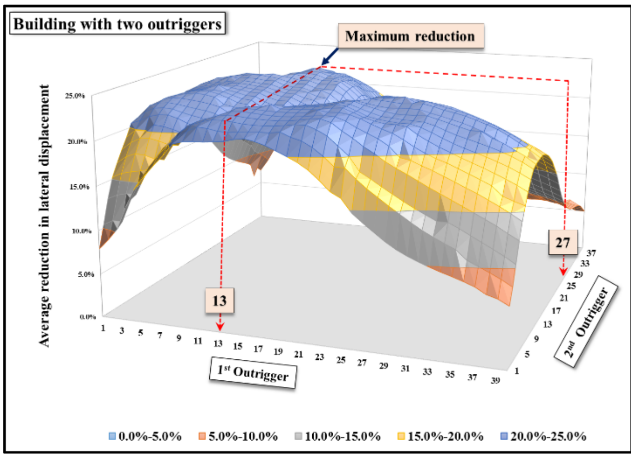

Fig. 3 Average reduction in top lateral displacement extracted from considered earthquakes versus the positions of the 1st and 2nd outrigger trusses

2.4 Depth of outrigger trusses

The choice of outrigger depth was determined according to a comparative study between different depths using the seven considered earthquake. Three depths for outrigger trusses at the predetermined optimum positions are examined when the outrigger depth equals one-storey height (h), two-storey height (2h), and three-storey height (3h). The average enhancement in lateral displacement from the seven earthquakes reaches 16.3%, 23.93%, and 27.6% for the depths h, 2h and 3h respectively for model with one outrigger while it reaches 24.4%, 36.28%, and 42.15% respectively in model with two outriggers as shown in Figs. 4(a)-(b). This clarify that outrigger truss with two-storey height gave significant enhancement in lateral displacement, especially in building with one outrigger truss. While increasing depth of outrigger truss to three-storey height gave small increasing in enhancement of lateral displacement. According to these results, the effective depth of outrigger trusses is chosen to be two-storey height. The final design for outrigger depth and position are summarized in Table 3.

The maximum lateral displacement and inter-story drift ratio of the design buildings with the optimum locations and depths for outrigger trusses from the linear time history analysis are shown in Figs. 5(a)-(c). It is obvious that the lateral displacement and inter-story drift ratio decreases with increasing the number of outrigger trusses in the model. The effect of outrigger in restoring lateral displacement is

Table 2 Summary of the selected earthquake records

Record ID	Earthquake	Station	Component	Magnitude	Duration (s)	PGA
EQ. 1	El Centro	Imperial Valley Irrigation District	S00E	6.9	53.76	0.35 g
EQ. 2	Loma Prieta	Oakland Outer Harbor Wharf Channel 1	270 DEG	6.9	39.98	0.276 g
EQ. 3	Loma Prieta	Corralitos, Eureka Canyon Rd.	0 DEG	6.9	40	0.629g
EQ. 4	Petrolia	Cape Mendocino Eq. Chan 3	0 DEG	7.2	59.98	0.589 g
EQ. 5	Northridge	Santa Monica City Hall Grounds Channel 1	0 DEG	6.7	59.98	0.37g
EQ. 6	Northridge	Century City, Lacc North	0 DEG	6.7	59.98	0.22g
EQ. 7	Imperial Valley	El Centro - Imperial Co. Center Grounds Chan 1	92 DEG	6.4	39.48	0. 315g

clear on its locations. This results from the reactions (tension-compression couple) that occurred in the outer columns and acted in the opposite direction to building movement. As a result the difference between upper and lower displacements of outrigger storey became very small causing the sudden reduction of inter-story drift at this location as shown in Figs. 5 (b)-(c). Figs. 6-7 represent the influence of outrigger on shear, and moment envelop for the second and third models divided by the maximum value in model without outriggers. It is found that the shear forces and bending moment decreases along the building height except at outrigger stories, which have significant increase in these internal forces. This occurs due to the existence of horizontal forces formed at outrigger stories (horizontal component of force created in inclined members of outrigger truss). The average shear force at outrigger stories from seven earthquakes reaches 74%, and 63% from maximum shear in model with one outrigger and model with two outriggers respectively. While, it reaches for bending moment 76.5% and 66.8% in model with one outrigger and model with two outriggers respectively. It is clear that when using only one outrigger in the building, it is exposed to very large forces so that it can withstand the rotation of the internal shear walls. Whereas, when using more than one outrigger, the forces generated in each one were lower and at the same time they gave greater improvement in lateral displacement as shown in Figs. 4-5. Moreover, the maximum shear and moment for most earthquakes occurred at outrigger story in model with one outrigger while they occurred at the base in model with two outriggers as shown in Figs. 6-7. Thus, increasing outrigger numbers enhances lateral displacement and reduces from sudden increase of internal forces on vertical members at outrigger floors and keep the place of maximum internal forces at the base of the buildings. To examine the effect of the leap in internal forces at outrigger storeys on failure modes of the considered models, they were studied when subjected to major or even destructive earthquakes using nonlinear time history analysis in the next sections.

3. Nonlinear Time History Analysis

To simulate plastic mechanism of the three-structural system considered, nonlinear time history analyses were

Table 3 Designed locations for outrigger trusses in the considered buildings

Considered buildings	No. of outrigger trusses	Position of outrigger
First Building	–	–
Second Building	1	at 22nd-23rd floors
Third Building	2	First outrigger at 13-14th floors Second outrigger at 27-28th floors

performed using ANSYS 15.0 software, (2013). These analyses are conducted on detailed finite-element models considering material nonlinearity and large deformations effects which taking into account stiffness changes resulting from change in element shape and orientation due to large deflection, large rotation, and large strain. Taking these effects in structural analysis had helped to initiate panel buckling and development of tension field action in TSPSW. To get accurate results, these effects had to be accompanied by applying load in small increments which was expensive in terms of solution time. The performance of the buildings was examined, first, under the design basis earthquake DBE and maximum considered earthquake MCE with return period 475 and 2475 years respectively that compatible to the construction area. After that, the ground-motion intensity was scaled up until the stress of any part of the models reached the ultimate value. El-Centro earthquake was used for this study. Finite-element models, simulation of building materials, responses of buildings under different intensities of earthquake, seismic capacity and failure modes were presented and discussed in the next subsections.

3.1 Finite element model

ANSYS 15.0 finite element software (2013) offers a lot of elements capable of modelling complex structures with nonlinear behavior. In this study, different types of elements were employed. BEAM188 was used to model the steel beams and horizontal members of outrigger trusses. BEAM188 are used also to model CFST columns by using built up sections. The diagonal members of outrigger trusses were modelled using LINK180. The web plate of thin steel plate shear walls (TSPSWs) was modelled

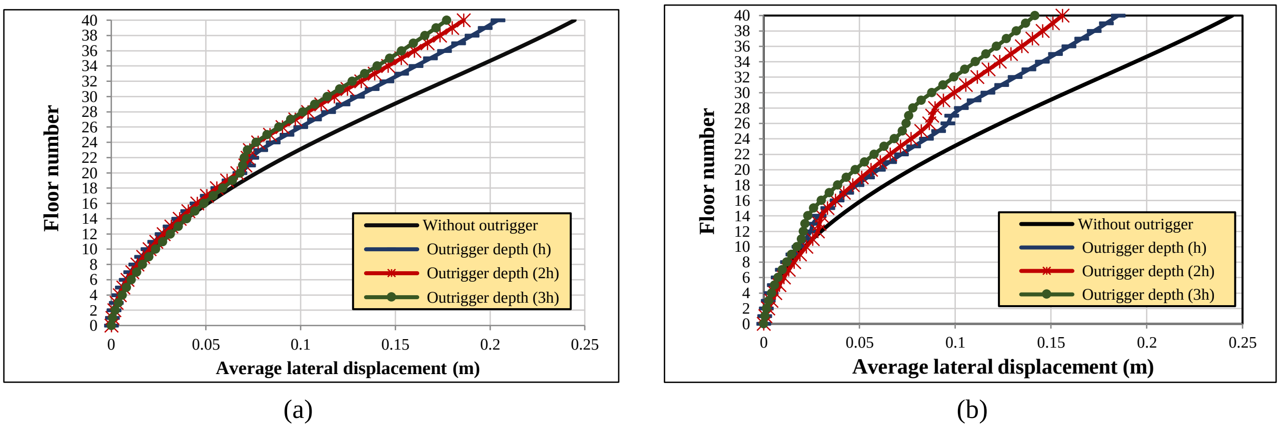

Fig. 4 Influence of outrigger depth on lateral displacement for (a) model with one outrigger truss and (b) model with two outriggers

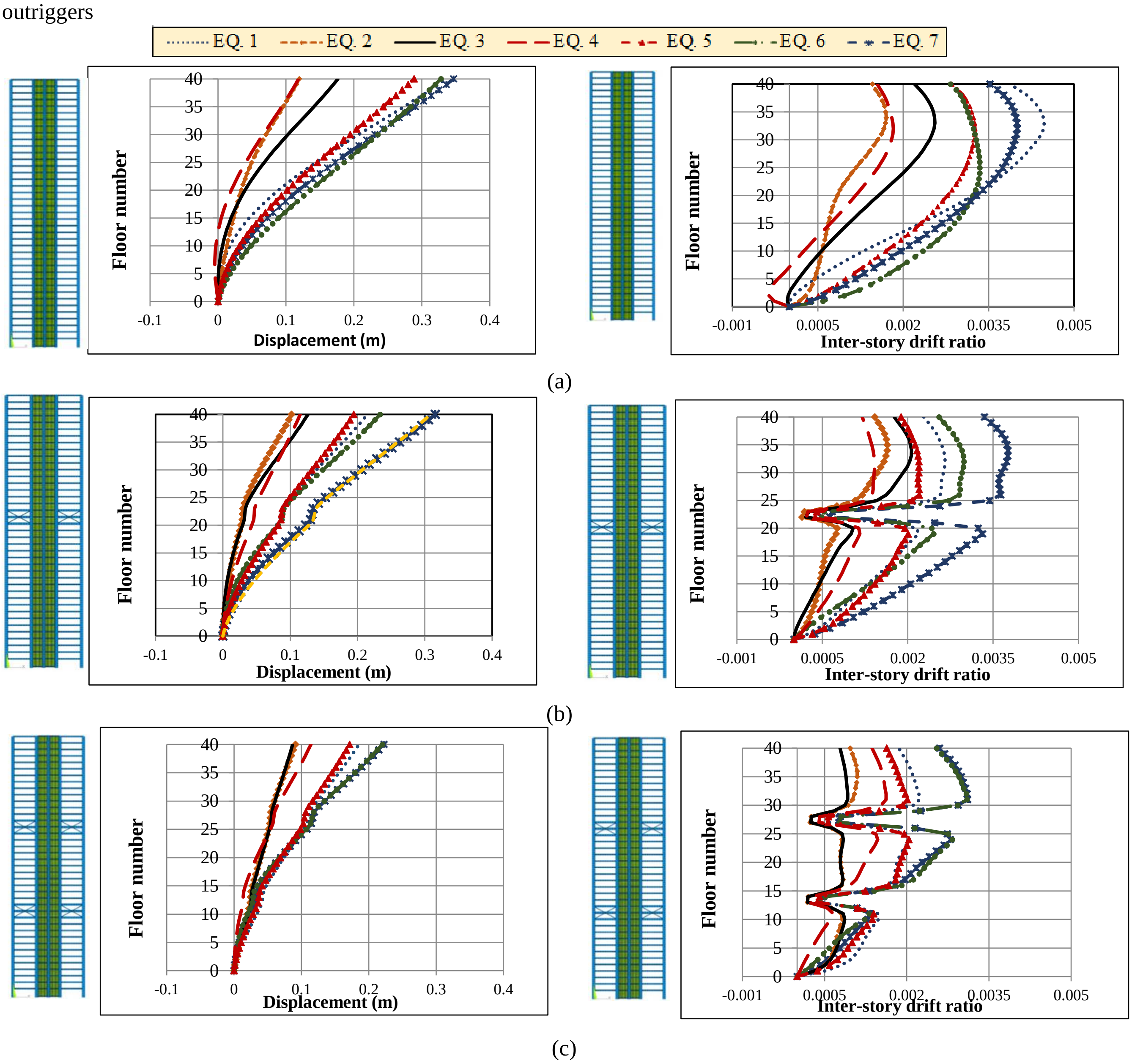

Fig. 5 Maximum lateral displacement and inter-story drift ratio for (a) model without outrigger, (b) model with one outrigger, and (c) model with two outriggers under seven different earthquakes

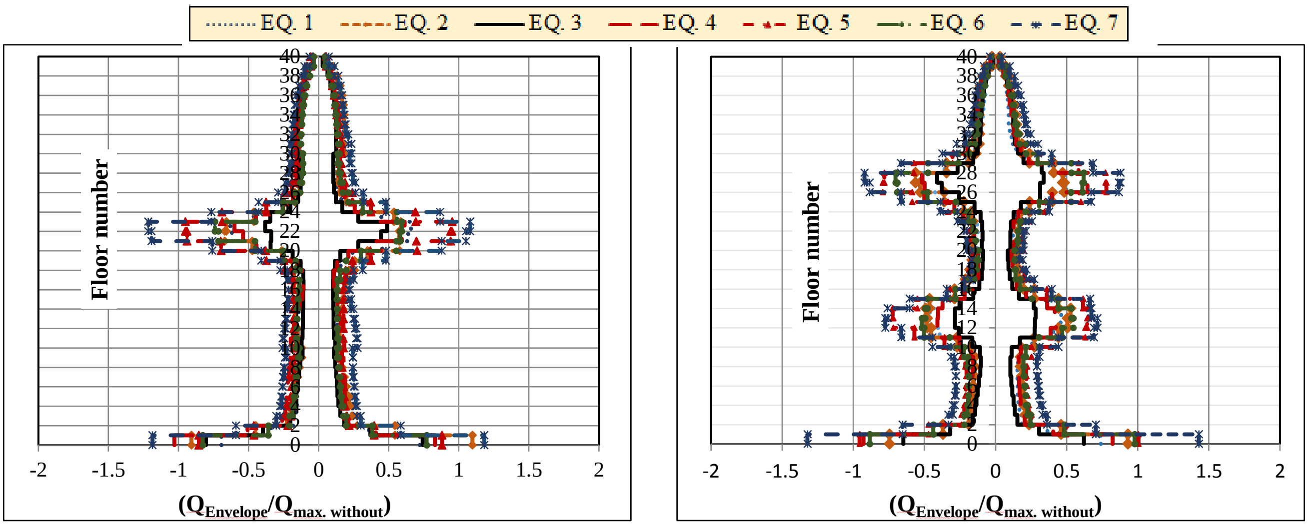

(a) (b)

Fig. 6 Shear envelops for; a) model with One Outrigger and b) model with Two Outriggers

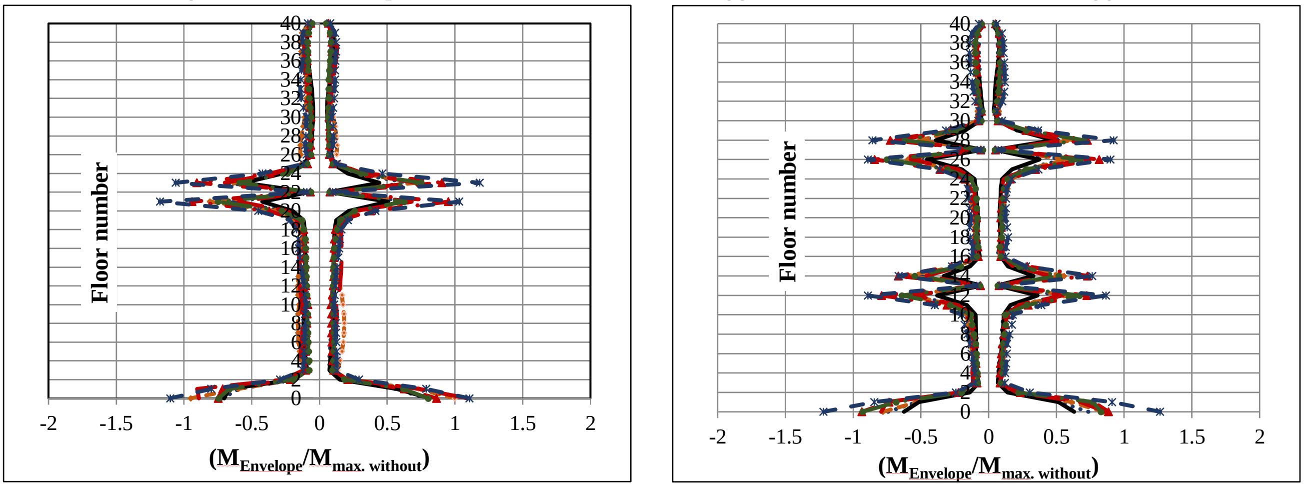

(a) (b)

Fig. 7 Bending moment envelop for; a) model with One Outrigger and b) model with Two Outriggers

using SHELL181 where it has many capabilities make it perfectly suitable for nonlinear analyses having large rotation, large strain effects or both. The composition of this element is based on true stress and logarithmic strain, and it take into consideration the effects of deformation due to transverse shear. In addition to, the kinematics of SHELL181 permit for stretching (finite membrane strains). The changes occur in thickness of element when it deformed are also taken into account during nonlinear analyses. All these capabilities are helped to simulate local buckling and tension field action in TSPSW during the full transient analysis (Time history analysis) that consider material and geometric nonlinearities. The connection between the building and its foundation was considered to be fixed. As indicated before, Finite-element analysis is a versatile and powerful tool but needs to be careful when dealing with it. Thus, sufficient pre-analyses were done to determine mesh size to achieve the most accurate and realistic results. Where, large sizes will give unreliable results while very small sizes will take more expensive time and storage for the analysis.

3.2 Material models

To simulate plastic mechanism of the considered structural system, two material models were used. Bilinear stress-strain relation with strain hardening 1%, according to EN 1993-1-5 (2006) was used for steel beams, outrigger trusses, web plate of steel plate shear walls and outer steel tube of CFST columns as shown in Figure 8 (a). Von Mises yield criterion with kinematic hardening rule was employed throughout the analysis. Steel grade S275, with yield and ultimate strengths equals 275 and 370 N/mm^2 respectively, was used for beams and web plate of TSPSWs, while steel grade S450, with yield and ultimate strengths equals 440 and 550 N/mm^2 respectively, was used for steel tube of CFST columns and outrigger members as illustrated in Table 1. For these steel grades, the Young's modulus and

Poisson's ratio were 210 GPa and 0.3 respectively. Rayleigh damping was adopted with a damping ratio of 2% for all models. The concrete type C40/50 was used for infill material of CFST columns. The confined stress-strain curve presented by EN 1992-1-1 (2004) which shown in Figure 8(b) was used to model the concrete core of CFST columns. In this curve the characteristic strength and strain of unconfined concrete were increased according to following equations.

$$f_{ck,c} = f_{ck}(1.0 + 5.0\frac{\sigma_2}{f_{ck}}) \qquad \text{for } \sigma_2 \le 0.05\, f_{ck}$$

or (5)

$$f_{ck,c} = f_{ck}(1.125 + 2.5\frac{\sigma_2}{f_{ck}}) \qquad \text{for } \sigma_2 > 0.05\, f_{ck}$$

$$\varepsilon_{c2,c} = \varepsilon_{c2}(\frac{f_{ck,c}}{f_{ck}})^2 \tag{6}$$

$$\varepsilon_{cu2,c} = \varepsilon_{cu2} + 0.2\frac{\sigma_2}{f_{ck}} \tag{7}$$

Where, $f_{ck,c}$,$\varepsilon_{c2,c}$, and $\varepsilon_{cu2,c}$, are compressive strength, strain at reaching maximum strength, and the ultimate strain of confined concrete. While, f_{ck}, ε_{c2}, and ε_{cu2}, are the same characteristics but for unconfined concrete. σ2 is the effective lateral compressive strength at ultimate limit state and can be calculated from empirical equations given by (Hu *et al*. (2003).

$$\frac{\sigma_2}{f_y} = 0.055048 - 0.001885(\frac{B}{t}) \quad \text{for } (17 \le \frac{B}{t} \le 29.2)$$

or (8)

$$\frac{\sigma_2}{f_y} = 0 \qquad \text{for } (29.2 \le \frac{B}{t} \le 150)$$

Thus, the stress-strain relationship of infill concrete was calculated to each cross-section of the CFST columns according to its dimensions and utilized in the finite-element analysis. The axial tensile strength for C40/50 is taking 3.5 N/mm^2 according to EN 1992-1-1(2004). The material failure criteria in ANSYS 15.0 (2013) is used to define the ultimate values of stress and strain in tension and compression.

3.3 Response of buildings under the design basis earthquake

Under the design basis earthquake (DBE), all models with and without outriggers acted in a linearly elastic manner where the stresses didn't reach values of yield stresses as shown in Fig. 9. Consequently, no plasticity occurred and this agreed well with the capacity design. The maximum stresses occurred in each model and their positions were illustrated in Fig. 9. It is obvious also in this figure that elastic buckling of the web panels occurs during the development of tension field action (TFA) in all cases. For the model without outrigger the maximum stresses occurred in bottom part of TSPSWs and it was close to the value of yield stress. In model with one outrigger the

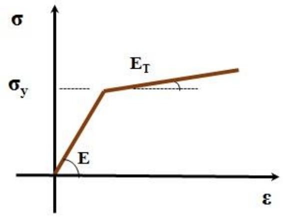

(a)

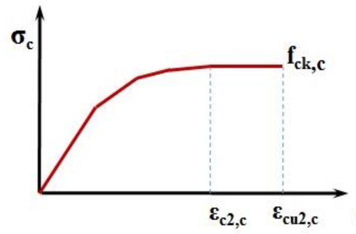

(b)

Fig. 8 (a) bilinear stress-strain relationships with strain hardening for steel, (b) stress-strain curve for confined concrete according to EN 1992-1-1(2004)

maximum stress in TSPSWs was about 88% of maximum stress of model without outrigger but its position was at outrigger floor due to the large increase in internal forces, caused by forces of outrigger members at this storey, when using one outrigger only as illustrated under linear analysis. Stress concentration was observed also in the connection between outrigger members and columns as shown in Fig. 9 (b). The model with two outriggers gives the smallest stress which equal 75.1% of maximum stress of model without outrigger and this occurred at the bottom part of TSPSWs. Moreover, by using two outriggers the stress was distributed in good manner between the column of TSPSW and external column as shown in Fig. 9 (c). In addition, the outrigger floor doesn't suffer from large stress as in model with one outrigger.

Fig. 10 shows the deformed shape of the three models at the time of maximum displacement for each one. This figure clarifies how outrigger works in the building, where at the outrigger stories; there was a restoration to lateral displacement. This was a result to the reactions (tension-compression couple) that occurred in the outer columns and acted in the opposite direction to building movement. The reduction in lateral top displacement in the model with two outriggers reached 30.1% in comparison with the model without outrigger and it reached 12 % for the model with one outrigger as shown in Figure 11(a). Figure 11 (b)-(d), shows the time history of base moment and base shear force of thin steel plate shear walls and axial reaction of external CFST columns respectively. The base moment of TSPSWs reduced after adding outrigger system to reach 89.86% and 80.74% of maximum moment of model without outriggers for the cases with one and two outriggers respectively. But on the other hand there was a slight increase occurred in base shear of TSPSW after adding outrigger trusses. This happened because of the extra stiffness from adding outrigger system. The maximum base shear occurred in the third model with two outrigger trusses, and it reached 4.3%

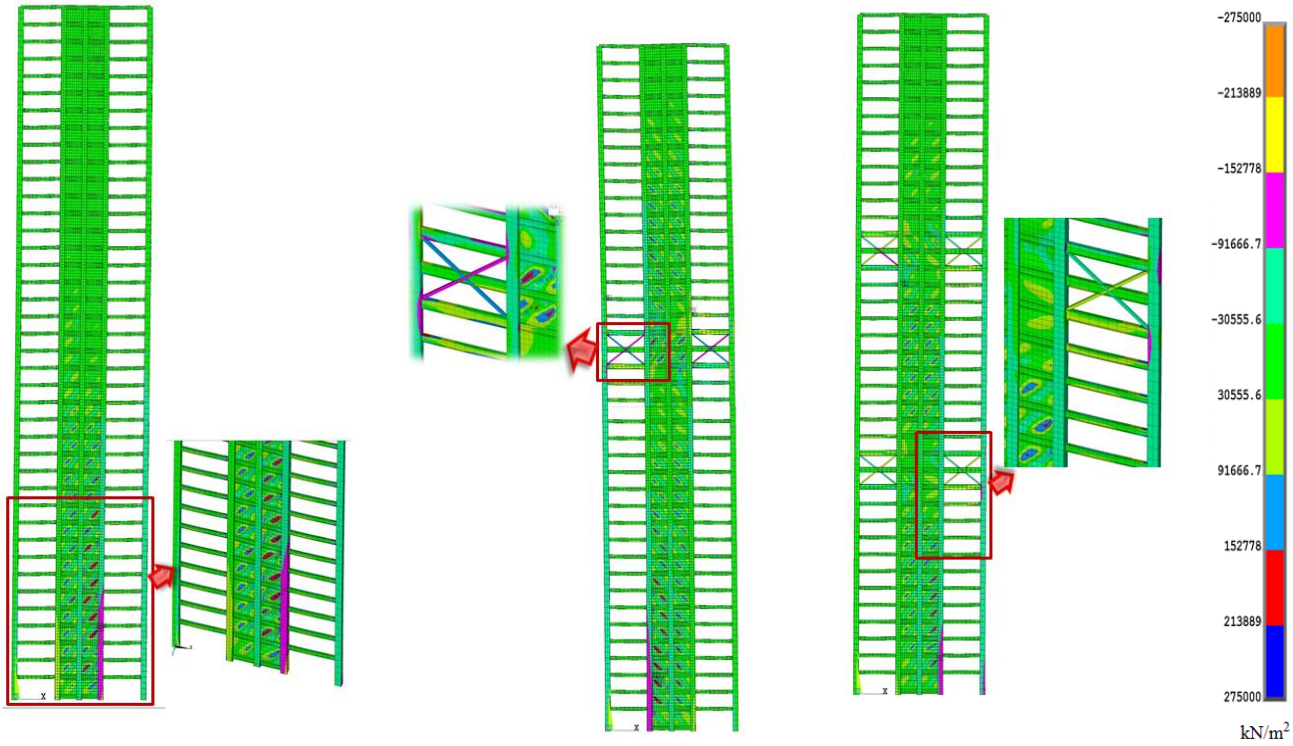

(a) (b) (c)

Fig. 9 Maximum Stress distribution and development of tension field actions in TSPSWs under design basis earthquake a) model without outrigger, b) model with one outrigger and c) model with two outriggers

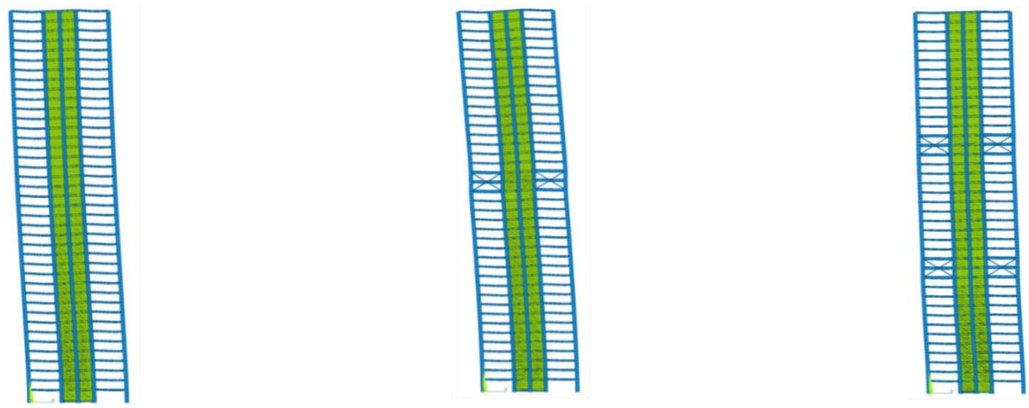

(a) (b) (c)

Fig. 10 Deformed shape at time of maximum displacement for each case a) model without outrigger, b) model with one outrigger and c) model with two outriggers

more than the model without outrigger while, in model with one outrigger the increase in base shear of TSPSWs reaches 1.8%. It is also observed that the external columns were subjected to a significant increase in axial force after adding outrigger system. The maximum increase in axial forces has reached 10.14% and 19.26% more than the model without outrigger for the second and third models respectively. This is due to the additional reaction coming from outrigger truss that caused redistribution of the forces between shear walls and external columns as it is clear in Fig. 9 (c). Where it reduces the axial forces on TSPSW columns and increases them on the external columns. This significant increase in axial forces of external columns associated with using outrigger should be taken into consideration in the design process of these columns.

3.4 Response of Buildings under the maximum considered earthquake

This section focuses on studying the performance of the models without outrigger, with one outrigger or with two outriggers through the nonlinear time history analysis under the MCE for the construction zone. The peak ground acceleration for this earthquake is calculated according to

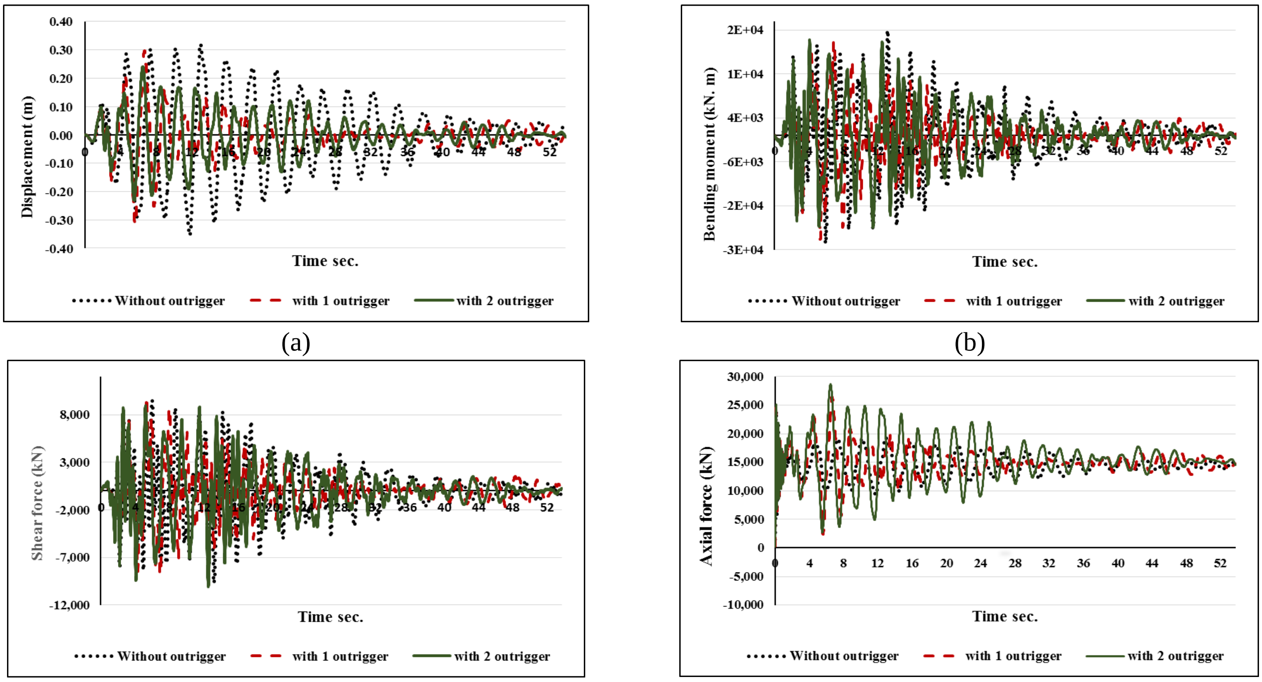

(a) (b)

(c) (d)

Fig. 11 Time history responses for the models without, with one and with two outriggers under the DBE earthquake, (a) Top lateral displacement, (b) Base moment of TSPSW, (c) Base shear of TSPSW, and(d) Axial force of CFST external column.

EN 1998-1 (2004) to achieve 2% probability of being exceeded within a 50-year period which corresponding to a return period of 2475 years. Thus, each model was analyzed under El Centro earthquake with normalized PGA equal to 0.433g. Under this earthquake the stress in lower part of TSPSWs in model without outrigger reached its ultimate strength in the left panel at the second story. This model presented a failure mode combining between yielding of the steel plate along the diagonal tension field in many positions in lower floors of TSPSWs, and plastic hinges formation in the ends of steel beams as shown in Fig. 12. Small lateral torsion buckling was observed in steel beams but, in actual building the lateral torsion failure mode will not be occurred due to the presence of the slab where lateral and torsional restraints are added to compression flanges with slab at the locations of plastic hinge to prevent deformation of the member as recommended by EN 1993-1-1(2006). Fig. 13 shows the formation and development of plastic strain in TSPSWs where, yielding was first observed in small areas in corners of infill plates in the 3rd, 4th, and 5th stories at time 2.2 sec. then it continued to spread along the diagonal tension field in most lower panels till time 6 sec. at which the stress of infill plate in the left panel at second story reached its ultimate value, initiating to plate damage at this position. The second model with one outrigger resisted this earthquake with limited damage where the stress for all of its components did not reach the ultimate value as shown in Fig. 14(a). Yielding of TSPSWs occurred at outrigger storey only but it didn't spread to other areas and didn't reach to ultimate strength till the end of the earthquake. This attributed to the large force occurred in outrigger members as explained before. The third model with two outrigger trusses gives superior performance at this

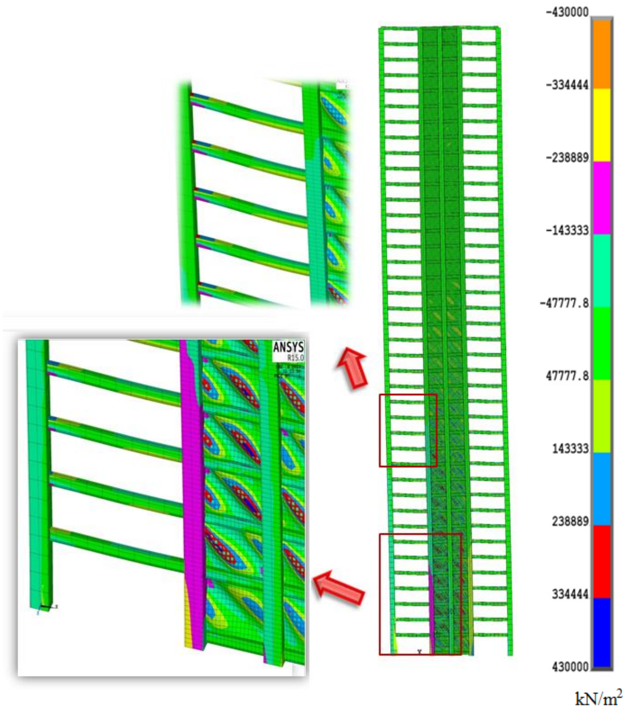

Fig. 12 Failure mode for model without outriggers under MCE with return period 2475 years

earthquake where the stresses of all of its components didn't reach their yield values as shown in Fig. 14(b). This confirms the previous result that, increase outrigger numbers reduces force produced by each outrigger, thus it reduces stress on TSPSWs at outrigger floors, in addition to, it gives more reduction in lateral displacement reaching 25.17% less than the second model as shown in Fig.15.

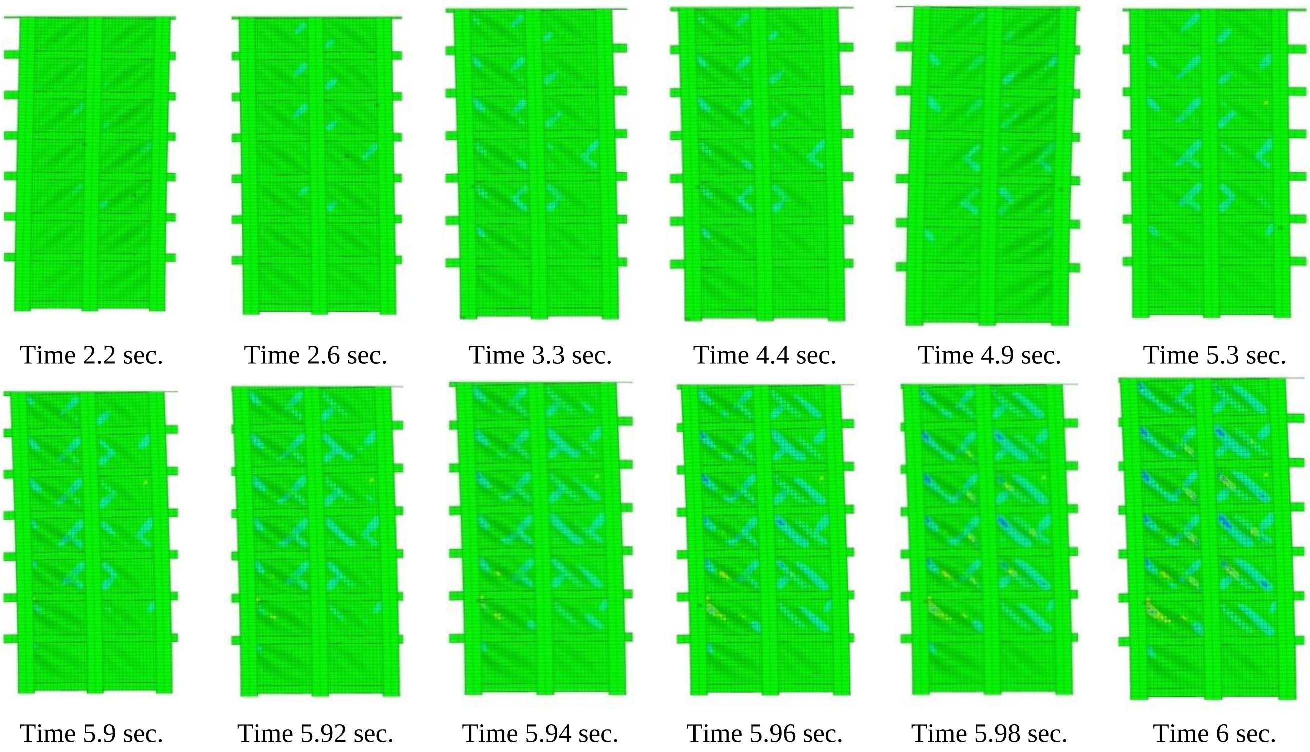

Fig. 13 Development of plastic strain in TSPSWs till the stress reaches its ultimate value

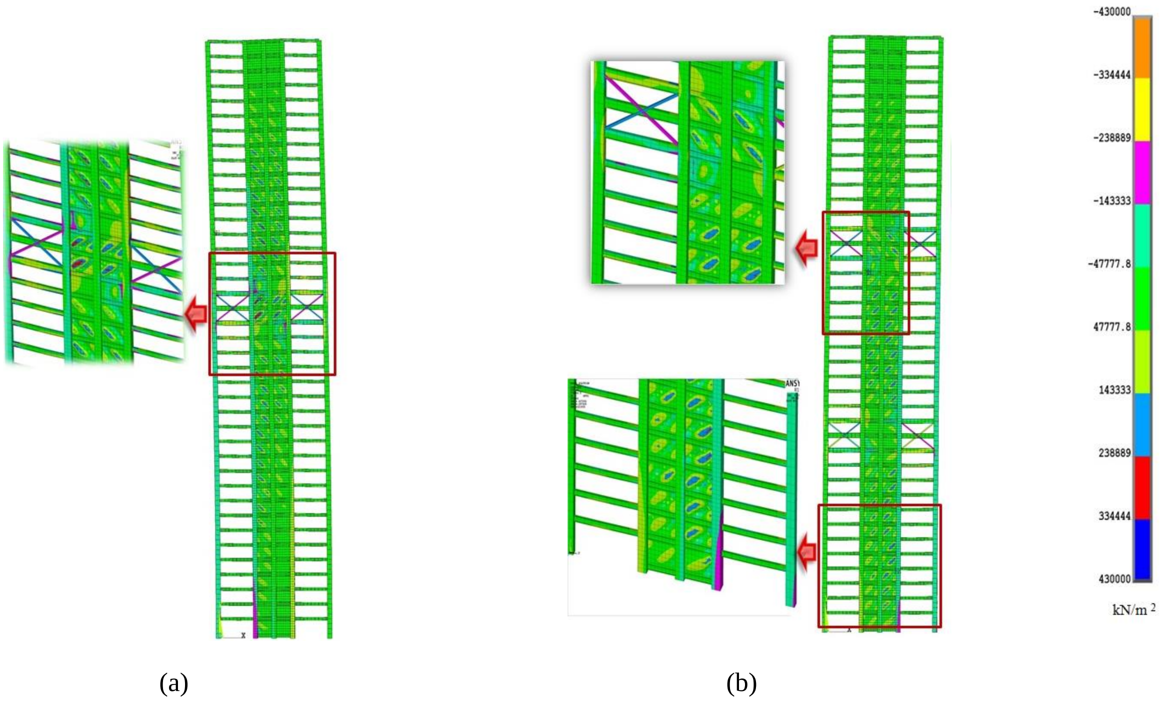

Fig. 14 Maximum stress distribution and tension field formation in TSPSWs under maximum considered earthquake for a) model with one outrigger, and b) model with two outriggers

3.5 Response of buildings under rare earthquakes

To find seismic capacity of the second and third model with one and two outriggers respectively, they analysed under increased levels of earthquake intensities till the stress of any part of the building reached the ultimate value. Under earthquake with PGA equals 0.5g, which represent 1.3% probability of being exceeded within a 50-year period and corresponding to a return period of 3797 year for the construction zone, the stress in the second model with one outrigger reached the ultimate strength. The main failure occurred on infill plate of TSPSWs at outrigger storey due to the high shear forces from outrigger members causing the plate reaching its ultimate strength as shown in Fig. 16.

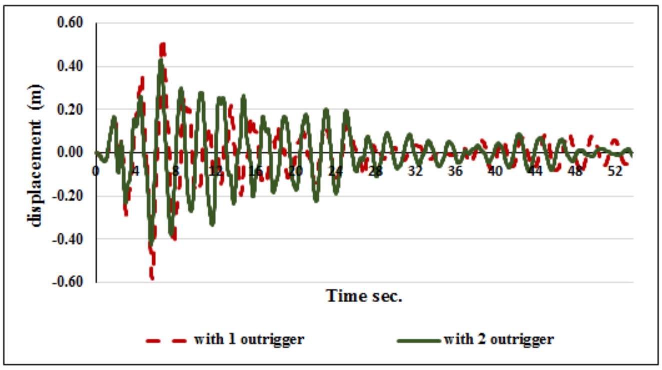

Fig. 15 Top lateral displacement time history for the models, with one and with two outriggers under the MCE earthquake

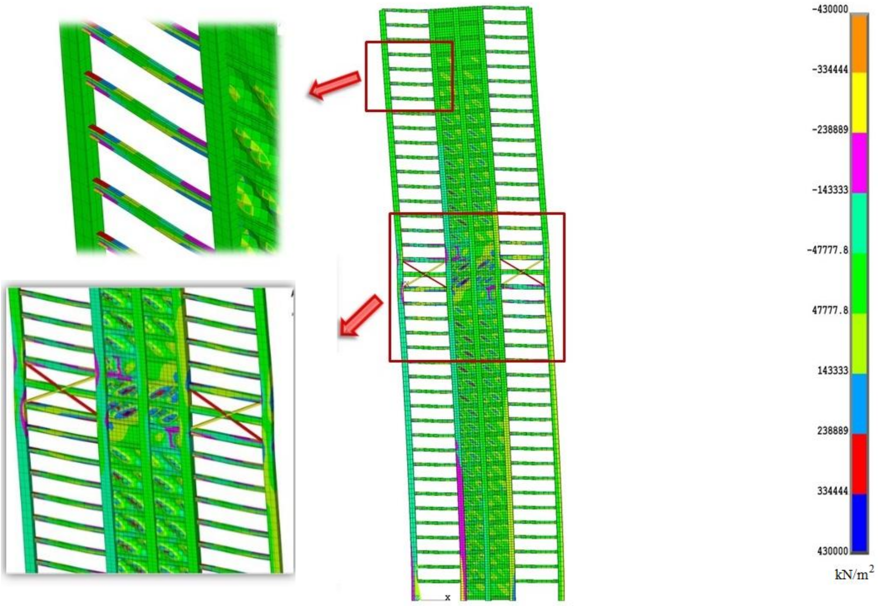

Fig. 16 Failure mode for model with one outrigger under earthquake with return period 3797 years

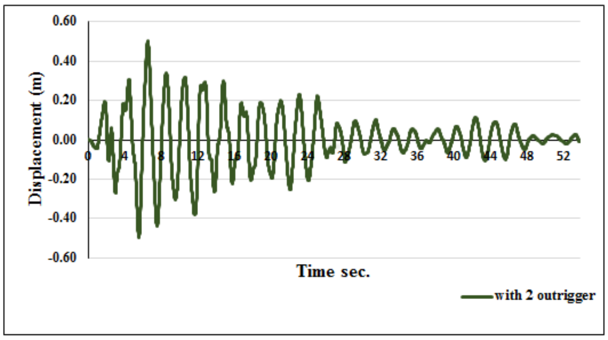

Fig. 17 Top lateral displacement time history for the model with two outriggers under earthquake with return period 3797 years

Yielding of the steel plate along the diagonal tension field was observed in many floors above and under outrigger floor. Moreover, high stress concentration was formed on CFST columns at connections with outrigger members which is not recommended as failure mode because it may cause crush for infill concrete but in this model the strain in infill concrete didn't reach ultimate compression strain. The steel beams in this model subjected to formation of plastic hinges as in model without outriggers. On the other hand, the third model with two outriggers resisted this earthquake without reaching ultimate values of stresses in all of its elements. Fig. 17 shows lateral top displacement in the model with two outriggers under El Centro earthquake with PGA equal to 0.5g. However, limited areas in infill plate of TSPSWs subjected to yielding at lower floors as shown in Fig. 18. The maximum stress didn't occur at outrigger floors and the stress concentration at connections between outrigger members and CFST was smaller than the model with one outrigger. This attributed to the smaller forces occurred in outrigger members when increasing their numbers along building height as illustrated previously. Under earthquake with PGA equal to 0.6g, which represent 0.763% probability of being exceeded within a 50-year period and corresponding to a return period of 6554 years for the construction zone, the stress in TSPSWs in model with two outriggers reached its ultimate value at lower floors. The main failure mode was infill plate damage across the entire panels at the bottom part of TSPSWs consisted of tension yielding and folds from buckling as shown in Fig.19. Moreover, plastic hinges at the ends of

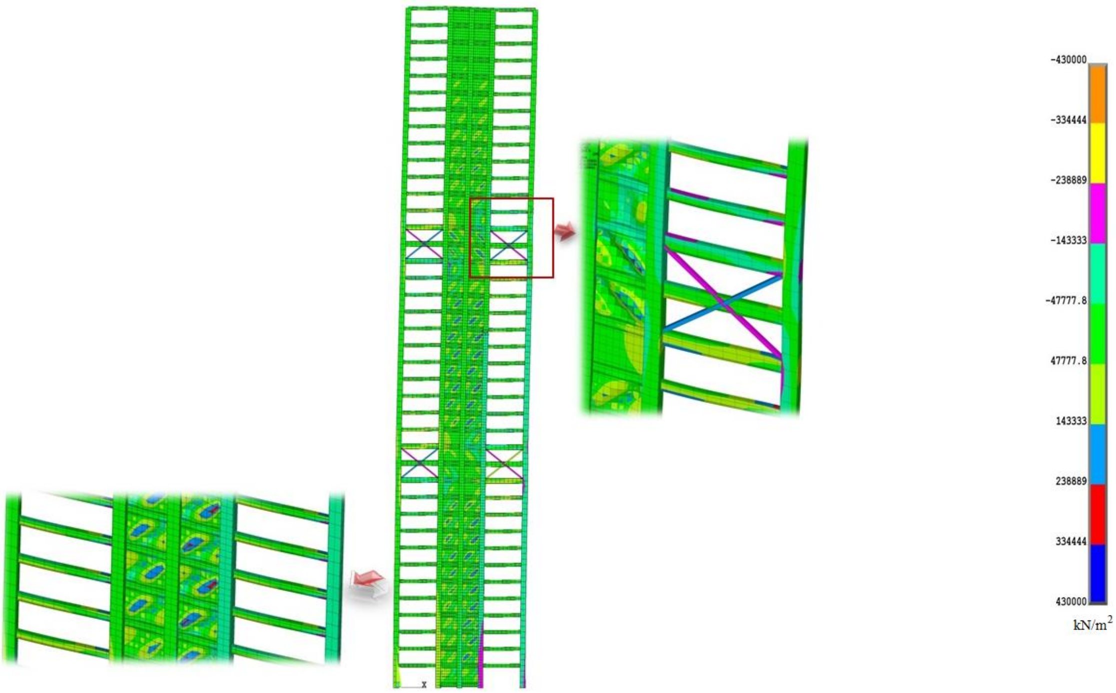

Fig. 18 Maximum stress distribution in model with two outriggers under earthquake with return period 3797 years

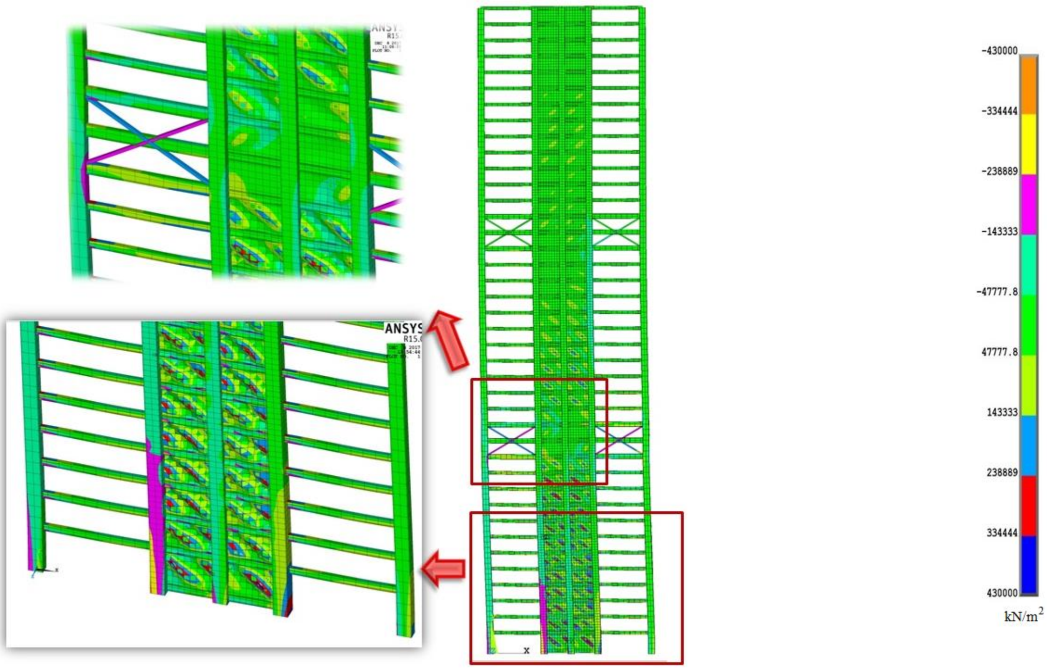

Fig. 19 Failure mode for model with two outriggers under earthquake with return period 6554 years

steel beams were formed. This failure mode is preferable because it gives suitable plastic mechanism under severe earthquakes. Moreover, the web of TSPSWs and the vertical members at outrigger storey exhibited small stress concentration in comparison with model with one outrigger.

As shown the model with two outriggers could resist till earthquake with return period equals 6554 years while the model with one outrigger and model without outrigger could resist till earthquakes with return periods equal 3797 and 2475 years respectively as summarized in Fig. 20. This indicate that, outrigger system improves significantly from seismic performance of the buildings where the seismic capacity of the model increased by 53.4%, and 164.8% more than the building without outrigger for model with one outrigger and model with two outriggers respectively.

4. Conclusions

The seismic performance of the dual system from of moment resisting frames and thin steel plate shear walls (TSPSWs) without, and with one or two outrigger trusses was studied in this paper. The responses, seismic capacity

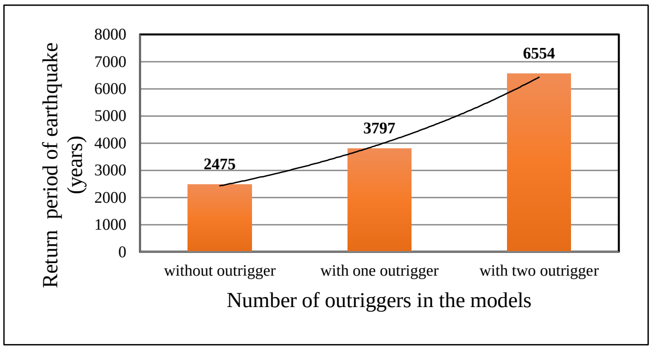

Fig. 20 Return period of earthquake at failure for the three considered models with different number of outriggers

and failure modes were derived through nonlinear time history analysis of detailed finite-element models using different earthquake intensities represented design, maximum considered and severe earthquakes. The main conclusions were summarized as follows:

- Adding outrigger to frame-thin steel plate shear walls system gave significant enhancement in lateral displacement and inter-storey drift ratio and this enhancement increases with increasing the depth and the number of outriggers along building height. This will encourage to use the TSPSWs, which have especial ability in dissipating energy during earthquakes, in tall buildings. The average enhancement in lateral displacement reaches 16.3%, 23.93%, and 27.6% for the depths h, 2h and 3h (h-story height) respectively in model with one outrigger while it reaches 24.4%, 36.28%, and 42.15% respectively in model with two outriggers
- Existence of outrigger system improve from seismic capacity of the considered structural system by about 53.4% and 164.8% more than the case without outrigger when added one and two outriggers respectively.
- Outrigger system causes leap in shear force and bending moment on vertical members around its floors. This occurs due to the existence of horizontal forces formed at outrigger stories (horizontal component of force created in inclined members of outrigger). This leap in internal forces decreases with increasing numbers of outriggers along building height because it reduces the forces generated in each one. The worst case was when using one outrigger only with TSPSWs where the maximum position of internal forces was at outrigger story not at the base as in case without and with two outriggers. This affect failure mode of the model with one outrigger where the steel plate of TSPSWs reaches its ultimate limit at this floor instead of the first floors as the cases without and with two outriggers.
- The failure modes for all cases were yielding of the infill steel plate along the diagonal tension field in TSPSWs in addition to plastic hinges in the ends of steel beams. Whereas the TSPSWs proved that it gives suitable plastic mechanism through earthquakes for all cases. The case with one outrigger exhibited high stress concentration on columns at outrigger story that may lead to brittle failure which is not recommended.

References

AISC 341-10 (2010), Seismic provisions for structural steel buildings, American Institute of Steel Construction, Chicago, IL.

ANSYS 15.0 (2013), ANSYS documentation; ANSYS Inc.

Behbahanifard, M.R., Grondin, G. Y. and Elwi, A. E. (2003) “Experimental and numerical investigation of steel plate shear wall”, Structural Engineering Report 254; Department of Civil Engineering, University of Alberta, Edmonton, Alberta, Canada.

Brunesi, E., Nascimbene, R. and Casagrande, L. (2016), “Seismic analysis of high-rise mega-braced frame-core buildings”, *J. Eng. Struct.,* **115**, 1-17.

Choi, I. R., and Park, H. G. (2008) “Ductility and energy dissipation capacity of shear-dominated steel plate walls.” *J. Struct. Eng.,* ASCE, **134**(9), 1495-1507.

Choi, I. R., and Park, H. G. (2009) “Steel plate shear walls with various infill plate designs.” *J. Struct. Eng.,* ASCE, **135**(7), 785-796.

Choi, H. S., Ho, G., Joseph, L. and Mathias, N. (2012) “Outrigger design for high rise buildings: an output of CTBUH outrigger working group”, CTBUH Technical Guide, Council on Tall Buildings and Urban Habitat, Chicago.

Choi, S.W., Kim, I. S., Park, J. H., Kim, Y., Sohn, H. G. and. Park, H. S. (2013), “Evaluation of stiffness changes in a high-rise building by measurements of lateral displacement using GPS technology”, *Sensors*, **13**(11), 15489-15503.

Chung, Y. L., Nagae, T., Hitaka, T. and Nakashima, M. (2010), “Seismic resistance capacity of high-rise buildings subjected to long-period ground motions: E-Defense shaking table test”, *J. Struct. Eng.*, **136**(6), 637–644.

Civalek, O. (2007), “Linear vibration analysis of isotropic conical shells by discrete singular convolution (DSC).” Structural Engineering and Mechanics, an Int'l Journal, **25**(1), 127-130.

Civalek, O. (2007), “Nonlinear dynamic response of MDOF systems by the method of harmonic differential quadrature (HDQ).” Structural Engineering and Mechanics, an Int'l Journal, **25**(2), 201-217

CSA-S16-09. (2009), Design of Steel Structures, Canadian Standards Association, Toronto.

Du, Y., Chen, Z. and Yu, Y. (2016), “Behavior of rectangular concrete-filled high-strength steel tubular columns with different aspect ratio”, *Thin-Walled Structures*, **109**, 304–318.

Du, Y., Chen, Z. and Xiong, M.X. (2016), “Experimental behavior and design method of rectangular concrete-filled tubular columns using Q460 high-strength steel”, *Constr. Build. Mater.*, **125**, 856–872.

Du, Y., Chen, Z., Liew, J.Y. R. and Xiong, M.X. (2017), “Rectangular concrete-filled steel tubular beam-columns using high-strength steel: Experiments and design”, *J. Constr. Steel Res.*, **131**, 1–18.

EN-1990 (2010), *Eurocode*, Basis of Structural Design. European Committee for Standardization, Brussels.

EN-1992-1-1 (2004), *Eurocode 2*, Design of Concrete Structures Resistance. Part 1-1: General rules and rules for buildings, European Committee for Standardization, Brussels.

EN 1993-1-1 (2005), *Eurocode 3*, Design of Steel structures. Part 1-1: General rules - General rules and rules for buildings, European Committee for Standardization, Brussels.

EN 1993-1-5 (2006), *Eurocode 3*, Design of steel structures. Part 1-5: General rules - Plated structural elements, European Committee for Standardization, Brussels.

EN-1994-1-1 (2004), *Eurocode 4*, Design of composite steel and concrete structures Resistance. Part 1: General rules and rules for buildings, European Committee for Standardization, Brussels.

EN-1998-1(2004), *Eurocode 8*, Design of Structures for Earthquake Resistance. Part 1: General rules, seismic actions and rules for buildings, European Committee for Standardization, Brussels.

Epackachi, S., Mirghaderi, R., Esmaili, O., Behbahani, A. A. T. and Vahdani, S. (2012), “Seismic evaluation of a 56-storey residential reinforced concrete high-rise building based on nonlinear dynamic time-history analyses”, *J. Struct. Design Tall Spec. Build.*, **21** (4), 233-248.

Fan, H., Li, Q.S., Tuan, A.Y. and Xu, L. (2009), “Seismic analysis of the world’s tallest building”, *J. Constr. Steel. Res.*, **65** (5) 1206-1215.

FEMA-350 (2000), NEHRP Recommended seismic design criteria for new steel moment frame buildings. Federal Emergency, Washington, D.C., USA.

FEMA-450 (2003), NEHRP Recommended Provisions for Seismic Regulations for New Buildings and Other Structures, Part 1: Provisions. Federal Emergency Management Agency, Washington, D.C., USA.

Gantes, C.J., Vayas, I., Spiliopoulos, A., Pouangare, C. C. (2001), “Bending and shear stiffness optimization for rigid and braced multi-story steel frames.” Steel and Composite Structures, an Int'l Journal, **1**(4), 377-392.

George A. Papagiannopoulos and Beskos, D. E. (2011), “Modal strength reduction factors for seismic design of plane steel frames.” Earthquakes and Structures, an Int'l Journal, **2**(1), 65-88.

Ghannadi, P. and Kourehli, S. S. (2019), “Model updating and damage detection in multi-story shear frames using Salp Swarm Algorithm.” Earthquakes and Structures, an Int'l Journal, **17**(1), 63-73.

Ashkezari G. D. (2018), “A performance based strategy for design of steel moment frames under blast loading.”

Earthquakes and Structures, an Int'l Journal, **15**(2), 155-164.

Gholipour, M. and Alinia, M. M. (2016), “Behavior of multi-story code-designed steel plate shear wall structures regarding bay width”, J. Constr. Steel. Res., **122**, 40-56.

Gunal, M. H. and Ilgin, H. E. (2014), *Tall Buildings Structural Systems and Aerodynamic Form, Routledge*, Taylor and Francis Group, London and New York.

Guo, L., Jia, M., Li, R. and Zhang, S. (2013), “Hysteretic analysis of thin steel plate shear walls”, *International Journal of Steel Structures*, **13**(1), 163-174.

Guo, H. C., Hao, J. P. and Liu, Y. H. (2015), “Behavior of stiffened and unstiffened steel plate shear walls considering joint properties”, *Thin-Walled Structures*, **97**, 53-62.

Hoenderkamp, J. C. D. and Bakker, M. C. M. (2003), “Analysis of high-rise braced frames with outriggers”, J. *Struct. Design Tall Spec. Build.*,**12** (4), 335–350.

Hoenderkamp, J. C.D. (2008), “Second outrigger at optimum location on high-rise shear wall”, *J. Struct. Design Tall Spec. Build.*, **17**(3), 619-634.

Hosseinzadeh, S.A.A. and Tehranizadeh, M. (2014), “Behavioral characteristics of code designed steel plate shear wall systems”, *J. Constr. Steel. Res.*, **99**, 72-84.

Hu, H.T., Huang, C.S., Wu, M.H. and Wu, Y.M. (2003), “Nonlinear analysis of axially loaded concrete-filled tube columns with confinement effect”, *J. Struct. Eng.*, **129** (10),1322-1329.

Ji, X., Kajiwara, K., Nagae, T., Enokida, R. and Nakashima, M. (2009), “A substructure shaking table tests for reproduction of earthquake responses of high-rise buildings”, *J. Earthquake Engng Struct. Dyn.*, **38** (12),1381–1399.

Jiang, H., Lu, X. and Zhu, J. (2012), “Performance-based seismic analysis and design of code-exceeding tall buildings in Mainland China”, *Struct. Eng. Mech.*, *Int. J.*, **43** (4), 545-560.

Lee, J., Park, D., Lee, K. and Ahn, N. (2013), “Geometric nonlinear analysis of tall building structures with outriggers”, *J. Struct. Design Tall Spec. Build.*, **22** (5), 454–470.

Lee, S. and Tovar, A. (2014), “Outrigger placement in tall buildings using topology optimization”, *J. Eng. Struct.,* **74**, 122-129.

Li, M., Lu, X., Lu, X. and Ye, L. (2014), “Influence of soil-structure interaction on seismic collapse resistance of super-tall buildings”, *J. Rock Mech. Geotech. Eng.*, **6**(5), 477-485

Li, Q. S. and Wu, J. R. (2004), “Correlation of dynamic characteristics of a super-tall building from full-scale measurements and numerical analysis with various finite element models”, *J. Earthquake Engng Struct. Dyn.*,**33**, 1311–1336.

Liew, J.Y., Xiong, M. and Xiong, D. (2016), “Design of Concrete Filled Tubular Beam-columns with High Strength Steel and Concrete”, *Structures*, **8** (2), 213–226.

lu, X., Chen, Y. and Mao, Y. (2012), “Shaking table model test and numerical analysis of a super tall building with high-level transfer storey”, *J. Struct. Design Tall Spec. Build.*, **21** (10), 699–723.

Lu, X., Su, N. and Zhou, Y. (2013), “Nonlinear time history analysis of a super-tall building with setbacks in elevation”, *J. Struct. Design Tall Spec. Build.*, **22** (7), 593–614.

Lu, Z., Chen, X., Lu, X. and Yang, Z. (2016), “Shaking table test and numerical simulation of an RC frame-core tube structure for earthquake-induced collapse”, *J. Earthquake Engng Struct. Dyn*., **45** (9), 1537–1556.

Meng, W., Weigum, Y., Yongjiu, S. and Jian, X. (2015), “Seismic behaviors of steel plate shear wall structures with construction details and material”, *J. Constr. Steel. Res.*, **107**, 194-210.

Park, H. S., Hong, K., and Seo, J. H. (2002), “Drift design of steel-frame shear-wall systems for tall buildings”, *J. Struct. Design Tall Spec. Build*, **11** (1), 35–49.

Patil, D. M. and Sangle, K. K. (2016), “Seismic Behaviour of Outrigger Braced Systems in High Rise 2-D Steel Buildings”, *Structures*, **8** (1), 1-16.

Purba, R. and Bruneau, M. (2014) “Seismic performance of steel plate shear walls considering various design approaches” Technical report MCEER-14-0005, Multidisciplinary Centre for Earthquake Engineering Research, State University of New York at Buffalo, Buffalo, New York.

Purba, R. and Bruneau, M. (2015), “Experimental investigation of steel plate shear walls with in-span plastification along horizontal boundary elements”, *J. Eng. Struct*., **97**, 68-79.

SAP2000 v15. (2010), Integrated software for structural analysis and design. Computers and Structures, Inc., Berkeley, CA.

Vatansever, C. and Yardimci, N. (2011), “Experimental investigation of thin steel plate shear walls with different infill-to-boundary frame connections”, *Steel Compos. Struct., Int. J.*, **11**(3), 251-271.

Vian, D. and Bruneau, M. (2005) “Steel plate shear walls for seismic design and retrofit of building structures” Technical report MCEER-05-0010, Multidisciplinary Centre for Earthquake Engineering Research, State University of New York at Buffalo, Buffalo, New York.

Wang, M., Shi, Y., Xu, J., Yang, W. and Li, Y. (2015), “Experimental and numerical study of unstiffened steel plate shear wall structures”, *J. Constr. Steel. Res.,* **112**, 373-386.

Wu, Y.T., Kang, D. Y. and Yang, Y. B. (2016), “Seismic performance of steel and concrete composite shear walls with embedded steel truss for use in high-rise buildings”, *J. Eng. Struct.*, **125**, 39-53.

Youssef, N., Wilkerson, R., Fischer, K. and Tunick, D. (2010), “Seismic performance of a 55-storey steel plate shear wall”, *J. Struct. Design Tall Spec. Build.*, **19**, 139-165.

Zeidabadi, N. A., Mirtalaeand, K. and Mobasher, B. (2004), “Optimized use of the outrigger system to stiffen the coupled shear walls in tall buildings”, *J. Struct. Design Tall Spec. Build.*, **13** (1), 9–27.

Zhou, Y., Zhang, C. and Lu, X. (2016), “An inter-story drift-based parameter analysis of optimal location of outriggers in tall

buildings", *J. Struct. Design Tall Spec. Build.*, **25**(5), 215-231.
Zirakian, T. and Zhang, J. (2015), "Structural performance of unstiffened low yield point steel plate shear walls", *J. Constr. Steel. Res.*, **112**, 40-53.

CC